UNITED STATES DEPARTMENT OF COMMERCE
JESSE H JONES, *Secretary*
CIVIL AERONAUTICS ADMINISTRATION
CHARLES I STANTON, *Administrator*
Technical Development Report No 31

THE DEVELOPMENT OF AN IMPROVED "STATION LOCATION" OR "Z" MARKER ANTENNA SYSTEM

By J C HROMADA and THOMAS A KOUCHNERKAVICH
CAA Experimental Station

FEBRUARY 1941

UNITED STATES GOVERNMENT PRINTING OFFICE
WASHINGTON 1943

TABLE OF CONTENTS

	Page
SUMMARY	1
INTRODUCTION	1
THEORETICAL DISCUSSION	2
EQUIPMENT	5
RESULTS	7
CONCLUSION	9
FIGURE INDEX	10

FIGURE INDEX

No		
1	Free space vertical radiation patterns for various numbers of elements, current ratios, and spacings	10
2	Vertical radiation patterns—present Z-marker array	11
3	Vertical radiation patterns—SDA array	11
4	Vertical radiation patterns—antennas a quarter wave above perfect earth	11
5	Plan layout of the SDA Z-marker antenna	12
6	SDA Z-marker antenna layout	12
7	Dipole antenna and tuning section	13
8	Dipole and support	13
9	Butt weld	13
10	SDA Z-marker antenna feeder system	14
11	Schematic diagram of SDA Z-marker antenna system	14
12	Common feeders, terminations and phasing section	14
13	UHF inner marker transmitter, audio oscillator, and voltage regulator	15
14	Antenna meter and probe detector	15
15	Schematic diagram of probe detector	15
16	Pick-up dipole	16
17	Pick-up dipole in place	16
18	Observed currents in pick-up dipole for various angular positions in the horizontal plane above the antenna	17
19	Marker receiving antenna on NC–17	17
20	Close-up of marker receiving antenna	17
21	UHF marker receiver and decade resistance box	18
22	UHF receiver calibration type RUG, serial No 14 Audio and indicator lamp volts vs radio-frequency input for various values of first intermediate-frequency stage cathode resistance	19
23	Esterline-Angus graphic meter	20

No.		Page
24	Calibration of Esterline-Angus graphic meter, Model AW, deflection vs input volts	20
25	Copies of actual flight recordings of the present Z-marker and the new SDA array at various altitudes showing comparisons of each array under identical flight conditions	21
26	Signal zone height determination	22
27	Z-marker patterns—measured zone widths for 10,000-foot signals	22
28	Z-marker patterns—measured zone widths for 10,000- and 20,000-foot signals	23
29	Parallel chord patterns of Z-markers for 10,000-foot signal	23
30	Z-marker patterns under condition of large crab angle	23
31	Horizontal pattern of SDA Z-marker for radial flights at altitudes of 500, 2,000, and 5 000 feet	24
32	Z-marker patterns—width in seconds—for 120 miles-per-hour ground speed	24

The Development of an Improved "Station-Location" or "Z" Marker Antenna System

SUMMARY

This report describes the development of an improved antenna system to be used with station-location or zone markers which designate points of reference or fixes, such as the cone-of-silence above a radio range station. The development of the antenna design based on theoretical radiation properties of spaced dipoles is given, the equipment used is described and the results obtained are analyzed. This antenna has been designated the "SDA" antenna (spaced dipole array).

The antenna system consists of two spaced dipole arrays at right angles to each other excited in quadrature time phase. Each array consists of cophased, spaced dipoles. The dipoles are of a simple standardized design which can be applied to other antenna systems such as fan markers or instrument landing system markers. The design of the dipoles and their geometrical lay-out are such as to insure excellent stability and reliability of operation throughout seasonal climatic changes. The construction of the antenna and its adjustment are not difficult. The gain of the new antenna over the present form of Z-marker antenna is two to one with respect to power input required for the same height of signal zone or a gain in signal zone height of 1.4 to 1 for the same power input into the two antenna systems. On the basis of a maximum signal zone height of 10,000 feet, the new SDA antenna system provides a signal zone considerably narrower than that of the present Z marker, being 46 percent as wide at a 500-foot altitude, 50 percent as wide at a 1,000-foot altitude and 68 percent as wide at a 3,000-foot altitude for radial on-course flights over the marker. With the SDA Z marker adjusted to produce a signal zone height of 20,000 feet (twice that of the present Z marker), the zone width does not exceed that of the present Z marker below 5,700 feet. Under these conditions, at 500 feet it is only 55 percent as wide as the present Z marker. At 1,000 feet it is 54.5 percent as wide and at 3,000 feet 74.5 percent as wide.

During flight conditions involving a large crab angle, the zone of the SDA antenna system is enlarged to a much less degree than the zone of the present Z-marker antenna.

The broad signal zone for parallel off-course flights at a 500-foot altitude is 79 percent of that obtained with the present Z marker. These desirable features will aid materially in increasing the accuracy of aircraft navigation during let-down procedures.

INTRODUCTION

The present "Station-Location" or "Z" markers used at radio-range stations to mark the cone-of-silence of the range are the result of development work which was carried on during the years 1934 to 1937. The first of the present commercially manufactured Z markers was installed and commissioned for regular service at Allentown, Pa., in April 1938. The description and flight test data on this installation are contained in Technical Development Report No. 14.[1] The experience gained in the past 2 years with the present Z markers has proved them to be a valuable complement to the Federal aids to air navigation. The demand for increased stability, greater accuracy as points of fix from which to begin the let-down procedure, and a greater height of signal zone[2] to insure reception

[1] W. E. Jackson and H. I. Metz, "The Development, Adjustment and Application of the Z Marker," Civil Aeronautics Authority, Technical Development Report No. 14, July 1938.

[2] "The term 'zone' is used to designate that region above the Z marker antenna in which can be found a signal of sufficient field strength to light the Z marker instrument light in an airplane. This region is often referred to as the 'light on' zone and is the useful region of the radiated beam.

at higher altitudes, has indicated that an improved antenna system would be desirable

THEORETICAL DISCUSSION

Greater stability of the Z-marker zone can be accomplished by an antenna structure which is more rigid mechanically than the one used at present Separating the individual elements of the antenna and their feeders to decrease their mutual coupling will facilitate the adjustment of the array and insure the stability of the final adjustment of the system An increase in altitude of the zone can be accomplished by increasing the power in the present antenna, but in so doing the radiated pattern will be expanded in all directions, resulting in a substantial broadening of the radiated beam at low altitudes The accomplishment of an increased altitude of zone with a narrower zone at low altitudes, necessitates redesigning the antenna system in order to provide greater vertical gain and sharper vertical directivity

Increasing the gain and directivity of antenna arrays by means of spaced antennas, reflectors (both driven and parasitically excited), and stacked arrays is well known to the art The utilization of these principles for the improvement of Z-marker antennas has been suggested by Green [3] Sharpness of vertical radiation may be obtained by using several rows of parallel dipoles spaced one-half wavelength apart in the rows and spacing the rows one wavelength apart Green shows that in order to obtain substantial symmetry between the radiation in the vertical plane containing the radiators and in the vertical plane at right angles to the radiators, the antenna array should form a square figure in the horizontal plane The numerical progression of rows of radiators and radiators per row is as follows 1–2, 2–4, 4–8, etc , respectively, where the first figure in the group indicates the number of rows and the second figure the number of radiators in each row The total number of radiators increases as 2^{2n-1} where n, an integer, may be considered the number designating the successive stages in the expansion of the system Thus, the third stage would require a total of 32 radiators, the 4–8 combination Aside from the difficulties of construction and adjustment of such a large number of radiators, the second stage of expansion, the 2–4 array, provides a vertical field pattern having two minor lobes which are 27 percent as large as the major lobe, a condition which nullifies its usefulness as a zone marker The 4–8 combination has six minor lobes, the greatest of which is approximately 23 percent of the major lobe A means of reducing the minor lobes offered by Green is to stack the antennas in the vertical plane Two layers of the 2–4 combination will double the number of radiators and reduce the secondary lobes to only 17 percent Three layers will triple the number of radiators and reduce the lobes to only 10 percent It can easily be seen that the system proposed is inherently complex mechanically and electrically

The late E J Sterba of the Bell Telephone Laboratories, in a memorandum of February 3, 1939, has shown that, in order to reduce the intensity of the minor lobes in a vertically stacked antenna system, it is necessary to feed the various stacked dipole elements of the array with currents of different amplitudes, which vary in accordance with the coefficients of the successive terms of the binomial expansion

$$(a+b)^n = a^n + \frac{n}{1}a^{n-1}b + \frac{n(n-1)}{1\times 2}a^{n-2}b^2 \text{ ---------etc}$$

where $(n+1)$=number of stacked dipoles in the array If the array consists of three stacked dipoles, $n=2$ and the relative amplitudes of the currents in the three dipoles would be

$$1+\frac{2}{1}+\frac{2(2-1)}{1\times 2} \text{ or } 1\text{-----}2\text{-----}1$$

For four stacked dipoles the relative amplitudes would be

1-----3-----3-----1

and for five stacked dipoles the relative amplitudes would be

1-----4-----6-----4-----1

An investigation was made to determine whether this principle of proportioned currents

[3] A L Green, "Marker Beacons for Symmetrical Radiation," Amalgamated Wireless (Australia) Technical Review, January 1938, vol 3, No 3, pp 113-142

could be applied to cophased, collinear dipoles to reduce the intensity of the minor lobes which result from the use of more than two dipoles spaced more than 180°

The free space radiation patterns in the vertical plane for several arrays of half-wave dipoles are shown in figure 1 and illustrate the application to spaced arrays of the principle of currents proportioned in accordance with the coefficients of the successive terms of the binomial expansion Figure 1 also shows the vertical patterns obtained with 2-, 3-, and 4-element arrays with unity current ratios Considering only dipole spacings of 180° the two-element array with equal currents has a substantially wide pattern with no minor lobes The addition of a third dipole in line, spaced 180° from an adjacent dipole and having a current amplitude equal to the other two dipoles, provides a sharper pattern but results in the addition of two minor lobes which are opposite in phase to the major lobe and have a maximum intensity of 11 7 percent of the major lobe radiation When the three dipole currents are proportioned in a 1–2–1 ratio, the minor lobes are entirely suppressed and the main lobe becomes slightly broader The major lobe sharpness may be increased by the use of four dipoles spaced 180° and carrying equal currents At an angle of 20° from the vertical, the strength of the radiated signal may be reduced to 55 4 percent of the value obtained with the three-element 1–2–1 array Minor lobes again develop which have a maximum value of 17 percent of the maximum of the major lobe These minor lobes may be eliminated, as before, by the proportioning of the dipole currents in a 1–3–3–1 ratio Although the minor lobes are eliminated the main lobe becomes somewhat broader, since the radiation at an angle of 20° from the vertical has been increased by 55 5 percent over that obtained with unity current in the four dipoles However, the signal strength of the 1–3–3–1 array at an angle of 20° from the vertical is 86 percent of the signal obtained from the 1–2–1 array

The radiation characteristic in the vertical plane which includes the elements of a four-element array with a 1–3–3–1 distribution of currents is practically the same as that of a three-element array with a 1–1–1 distribution of currents, except that the minor lobes have been suppressed The sharpening of the pattern can be carried on further by the addition of more dipoles and by the proper proportioning of the currents The selection of the desired array becomes a problem of economy and compromise In general, the intensity of the minor lobes increases with increase in the number of radiators unless the currents are properly proportioned In actual service, where the radiators are located a quarter wavelength above a metallic counterpoise, the free space radiation characteristic will be modified by the factor

$$\sin (90 \sin \theta)$$

It is possible to design an array in which the minor lobes are only partially suppressed below a tolerable value However, the limit of expansion of the array is governed by cost and space limitations, which increase with an increase in the number of dipoles In this development it was decided to limit the array to four dipoles

A study was then made to determine the limits to which the radiation pattern could be sharpened by spacing the elements of the array at distances greater than 180° Figure 1 also illustrates the patterns obtained from the 1–2–1 array with dipole spacings of 180°, 200°, 220°, and 240° It is seen that as the spacing increases, the pattern becomes sharper with a slight tendency toward the production of minor lobes It is interesting to observe that the 1–2–1 array, using 220° dipole spacing, has a sharpness equal to the 1–3–3–1 array, using a spacing of 180° The maximum value of the minor lobe obtained with the 1-2–1 array and 220° spacing is only 1 6 percent of the maximum value of the major lobe for free space radiation This is reduced to 0 64 percent when the array is located a quarter wave above a metallic counterpoise A spacing of 240° shows a slightly sharper main lobe pattern with 4 1 percent minor lobes for free space radiation The minor lobe amplitude reduces to 2 2 percent when the array is located a quarter wave above a metallic counterpoise The minor lobes are present

with spacings of 200° and 220°, but they are too small to be indicated on the polar coordinate paper

Figure 1 shows patterns for free space radiation Subsequent radiation patterns differ from those shown in figure 1 in that the reflections from the earth's surface, assuming perfect conducting ground, are taken into consideration Also, in figures 1 to 3, the radiation patterns have all been plotted to a maximum of unity at 90° from the horizontal plane The patterns, therefore, do not show the gain of one array over the other and are not comparable on the basis of constant power input to the arrays The numerical figures shown above the radiators on the figures are relative amplitudes of the current values in the elements of each array

Figure 2 shows the pattern for the Z-marker array in present use at radio range stations The array consists of two collinear, cophased dipoles carrying equal currents and spaced 180° In addition to the radiation pattern, $f_1(\theta)$ in a vertical plane containing the radiators, the radiation pattern $f_B(\theta)$, in a vertical plane normal to the line of the radiators, also is shown These planes henceforth will be referred to as the A and B planes The solid of radiation would resemble a thick cactus leaf and the distance from the origin to any point on its surface would represent the relative field strength at that particular angle measured at a constant distance from the origin The direction of the electric potential vector at any point is at all times in a plane containing the radiators and the point in question, and is normal to the line joining the point with the origin Thus, in the A plane the direction of the electric potential vector varies from vertical at the earth's surface to horizontal above the array In the B plane the electric vector is at all times horizontal and parallel to the radiators Since airplanes usually fly through the marker zones at a constant altitude with the receiving antenna in a horizontal position, the patterns shown are not strictly representative of the voltage impressed on the receiving antenna as it is flown over the array However, at high altitudes and near a point directly over the array the effect of varying distance can be neglected When an airplane is flying in the A plane, the $f_1(\theta)$ pattern is to be considered, with proper emphasis being given to the angle between the electric potential vector and the receiving antenna The voltage impressed on the receiving antenna is the product of the field strength and the cosine of this angle The effect of this factor, which is equal to $\sin\theta$, where θ is the elevation angle measured from the horizontal is to sharpen the $f_A(\theta)$ pattern at low angles with only a slight effect at the high angles When the airplane is flown parallel to the A plane and to one side of the array, the solid radiation pattern must be considered However at the instant it enters the B plane, the $f_B(\theta)$ pattern without modification represents the voltage impressed on the receiving antenna, since the electric potential vector is parallel to the receiving antenna When these factors are borne in mind, figure 2 indicates that an airplane flying parallel to the array and to one side of a point directly over the antenna will enter a signal zone of sufficient intensity to give a "light-on indication at a greater distance to one side of the station than would be the case had the airplane flown through a point directly over the station This phenomenon of the elongation of the "light-on zone for flights parallel to the array and to one side results in a broad indication of the location of the Z marker To reduce this broadening of the "light-on' zone, it is necessary to make the $f_B(\theta)$ pattern simulate the $f_1(\theta)$ pattern as much as possible, neglecting, of course, the pattern of the receiving antenna Although the $f_A(\theta)$ pattern of the 1–2–1 array (with 220° spacing) was considered satisfactory, its $f_B(\theta)$ pattern is identical with the $f_B(\theta)$ pattern of figure 2 To reduce the $f_B(\theta)$ pattern, the array was modified in such a manner as to obtain the electrical equivalent of the 1–2–1 array and thus maintain the $f_1(\theta)$ pattern This was accomplished by splitting up the center element into two parallel dipoles, spaced 180° and carrying equal currents The net result is a four-dipole array, a plan view of which is shown in figure 3 The $f_A(\theta)$ and $f_B(\theta)$ patterns are illustrated in the same figure The minor lobes of the $f_A(\theta)$ pat-

tern are too small (0 64 percent) to be drawn on polar coordinate paper Figure 4 shows the patterns of figures 2 and 3 plotted in rectangular coordinates, and gives a clear picture of the degree of sharpness effected by the SDA array It is also seen from figures 2, 3, and 4 that the sharpening effect, through the use of the SDA array design, has been greater in the $f_A(\theta)$ patterns than in the $f_B(\theta)$ patterns Figure 4 also indicates that the present Z marker is more symmetrical than the SDA array In practical terms this signifies, as will be shown later in discussion of the results, that the reduction in the elongated pattern, though substantial, was not so great as the reduction in the zone width

During the early stages of development of this array, the end dipoles were also displaced so that each one was collinear with one of the center dipoles This arrangement resulted in a greater narrowing of the $f_B(\theta)$ pattern than that obtained with the final arrangement, and a greater reduction in the elongated pattern when flying parallel to the array and to one side However, because of the arrangement of dipoles, the array was not symmetrical for angles measured either side of the normal to the collinear axis of the array in the horizontal plane This dissymmetry resulted in a minor lobe of 17 5 percent for radial flights over the array in a plane which made a 120° angle with the axis of the array The maximum of the lobe occurred at an elevation angle of 27 5° At 40° it is still 12 percent Thus this minor lobe is quite apparent both in the headset and on the marker indicator lamp for parallel chord flights to either side of the array at an altitude of 500 feet For this reason this arrangement was discarded This arrangement is sometimes referred to as the unsymmetrical SDA array (see fig 30) and can be seen in figure 17 The final arrangement of the Z marker is referred to as the symmetrical SDA array and has a minor lobe of 5 65 percent for a 45° radial flight through the marker However, this lobe lies along a 21° elevation angle The horizontal distance for an altitude of 500 feet at 21° elevation angle is 1,374 feet Examination of the elongated patterns in figure 29 will show that this distance out along a 45° radial is well outside the "light-on" zone of the marker As the airplane is moved in nearer the array, the elevation angle increases This fact may explain why no minor lobes are detected on parallel chord flights at an altitude of 500 feet either side of the symmetrical SDA array The general equation for this array is

$$F(\theta)_\alpha=\frac{1}{2}[\cos(A\cos\theta)+\cos(B\cos\theta)]\left[\frac{\cos(90^\circ\cos\alpha\cos\theta)}{\sqrt{1-\cos^2\alpha\cos^2\theta}}\right][\sin(90^\circ\sin\theta)]$$

where $A=220^\circ\cos\alpha$

$B=90^\circ\sin\alpha$

θ=the elevation angle measured from the horizontal plane

α=the angle the vertical plane under consideration makes with the collinear axis of the array

The first term of $F(\theta)_\alpha$ is the array factor, the second the form factor of the dipoles, and the third the reflection factor of the ground or counterpoise

EQUIPMENT

The SDA antenna consists of two of the arrays shown in figure 3 placed at right angles and fed in quadrature time phase with respect to each other Each array consists of the equivalent of three collinear cophased spaced dipole radiators separated 220° and having current ratios of 1–2–1 The central equivalent element is two dipoles spaced one-half wavelength apart laterally with each carrying unity current This layout is shown in figure 5 Dipoles 1, 2, 3, and 4 constitute one array while radiators 5, 6, 7, and 8 constitute the other array The dipoles are supported a quarter wavelength above a 30-foot-square counterpoise consisting of three-inch-square wire mesh supported 6½ feet above ground The counterpoise is similar to the present Z-marker counterpoise Figure 6 shows the complete layout of the antenna system For this photograph the elements were painted with aluminum paint so that they would stand out against a dark background

All radiating elements of the experimental antenna consist of horizontal dipoles of seven-

eighths inch OD copper tubing supported at their centers by Isolantite insulators in Raybould tee junction boxes The antennas are fed through 140-ohm dual conductor shielded transmission line A schematic diagram of a dipole and feeder is shown in figure 7 The dipoles are fed at a point of low potential and thus are inherently free from insulation difficulties and make for a stable system which is little affected by rain, snow or ice Figure 8 shows an assembled dipole in place, supported on a galvanized steel pedestal Feeder connections are made below the level of the counterpoise

All three-way and right-angle junctions of the two-wire transmission line were made by butt soldering the lines with silver solder Figure 9 shows a butt tee junction

Figure 10 is a view of the feeders under the counterpoise A spread-out diagram of the system is shown in figure 11 The two right-angle sections of the antenna system are designated array *A* (dipoles 1, 2, 3, and 4) and array *B* (dipoles 5, 6, 7, and 8) Building-out sections of transmission line *TA* and *TB* are used to terminate the main feeders to the two arrays The main feeder to array *B* is 90° longer than the feeder to array *A*, to provide the necessary quadrature phase relationship The termination of the two common feeders and the 90° phasing section are shown in figure 12

Radio-frequency power was supplied to the antenna by a 75-megacycle, 5-watt transmitter, type TZE A 3,000-cycle modulation voltage was applied from an external source Figure 13 shows the transmitter, its voltage regulating transformer and a 3,000-cycle audio oscillator set up in a house under the counterpoise At the right side of the figure can be seen the end of the shielded transmission line terminated in an Isolantite end seal

The measuring instruments used in adjusting the antenna and feeders consisted of a probe detector, clip-on antenna meter and a pick-up dipole The probe detector, figures 14 and 15, was used to measure voltages on the conductors of the transmission lines Slotted sections of shielding made it possible to make measurements on the transmission line conductors The slotted sections were replaced with solid shielding after the measurement had been completed The meter used to measure the currents in the dipoles was a Western thermo-milliammeter, 0–120, and is also shown in figure 14 The meter terminals are shunted with 0–75 micromicrofarad variable condenser for tuning out the inductance of the meter To measure relative dipole currents and balance of currents in the two halves of the dipoles, the meter was clipped on the dipole on either side of the Raybould tee junction The pick-up dipole, figure 16, was used to measure the radiated field above the antenna at various angles in the horizontal plane to indicate the circularity of polarization of the radiated field The dipole was made of two sections of telescoping tubing to facilitate tuning, and the received current was read on a thermo-milliammeter, 0–120, connected at its center The wheel attached to the assembly was used to rotate the dipole through 360° by means of a wrapped cord, manipulated from ground Figure 17 shows the dipole in place approximately 12 feet above the antenna The layout of the dipoles seen in this figure is one which preceded the final layout shown in figure 5 and has been referred to above as the unsymmetrical SDA array Figure 18 is a plot of the current in the pick-up dipole for various angular positions in the horizontal plane Since the pick-up dipole is relatively close to the transmitting antenna and is directly over it, where the electric field in the *A* and *B* planes is equal, the circular pattern obtained from the readings, therefore, is a measure of the equality of the currents in the radiators of the two arrays and of their quadrature phase relationship

Civil Aeronautics Administration airplane NC–17 was used in testing the SDA marker antenna and for obtaining comparative data from the present Indianapolis (ID) Z-marker antenna This airplane is a Waco, Model N biplane The receiving antenna on NC–17 is a standard Z-marker dipole receiving antenna mounted under the fuselage of the airplane and collinear with its longitudinal axis The antenna details are shown in figures 19 and 20

The marker receiver installed in NC–17 is a type RUG receiver built by the Western Elec-

tric Co (their type No 27A) This receiver is described in Western Electric Bulletin 912A The gain of the receiver was made adjustable by substituting a decade resistance box for the variable control circuit in the cathode of the first intermediate frequency stage Figure 21 shows the receiver and the decade box The resistance of the decade box can be adjusted to limit the gain of the receiver and thus the height of the signal zone The linearity of the receiver was investigated and the results are shown in figure 22 These curves show the audio output voltage vs radio-frequency input, modulated 30 percent with 3,000 cycles, for several values of resistance in the cathode circuit of the first intermediate-frequency stage The signal generator was not capable of 100-percent modulation, which is used for all marker transmitters The marker-lamp voltage for various radio-frequency inputs and various values of resistance in the first intermediate-frequency stage cathode circuit also is plotted in figure 22 In measuring the lamp voltage, a 10-ohm resistor was inserted in the common return to all three indicator lamps provided with the receiver to simulate the normal condition of the circuit in airplane NC–17 This resistor is used in the airplane circuit to reduce the residual current in the indicator lamps when there is no received signal From the curves it can be seen that if the output audio voltage is kept below 13 volts and the output lamp voltage is kept below five volts, the receiver will be essentially linear in operation

An Esterline-Angus 0–5 milliampere Model AW graphic recorder figure 23, was used to record either the audio output of the receiver or the voltage applied to the indicator lamp The audio output, selected by a double-pole double-throw toggle switch, was applied to the recorder through a 2,000-ohm potentiometer and a copper oxide rectifier The indicator lamp voltage was measured through a 302-ohm resistor The calibration of the recorder is shown in figure 24 A 120-cycle voltage was used in calibrating the lamp circuit and a 3 000-cycle voltage was used to calibrate the audio circuit

RESULTS

The power into the SDA Z-marker antenna was adjusted to produce the same height of signal zone as that obtained from the present Indianapolis (ID) Z marker, and the gain of the receiver was adjusted so that the height of the signal zones of both markers was limited to approximately 10,000 feet above ground Comparison flights were then made on the two markers and the width of the "light-on" zone was measured Direct measurements of the light time with a stop watch were not considered accurate since the apparent brilliancy of the light is affected by the normal lighting in the airplane cabin, thus making it difficult to judge the exact brilliancy at which to begin and end the timing It was therefore found expedient to measure the light time by means of the Esterline-Angus recorder The 3,000-cycle tone output of the receiver was rectified and applied to the recorder The time during which the rectified signal voltage was equal to or greater than a predetermined value was scaled from the chart recording, which moves through the recorder at a constant speed The value of rectified voltage at which the time axis was established is equal to the maximum value of rectified voltage recorded at the top of the signal zone, viz, 10,000 feet The width of the signal zone as measured in time was converted to distance in feet from readings of the indicated air speed, taking into account the proper correction factors for temperature altitude, wind direction, and wind velocity

Sample recordings of the signal zones of both Z markers for altitudes from 1,000 to 9,000 feet are shown in figure 25

The height of the signal zone was obtained from recorder deflections taken on flights over the marker at two or more altitudes which are sufficient to insure linear operation of the receiver The maxima of the deflections were then plotted for various altitudes and a straight line was drawn through them The altitude at which this line intersects the value used as a light time axis is the height of the signal zone Curve *A* of figure 26 illustrates such a signal height determination This curve intersects the light time axis at an altitude of 8,800 feet It will be noted that at low altitudes the region of strong signal strengths, the maximum de-

flections are limited to eight units by the action of the automatic volume control of the receiver The straight portion of curve A was extrapolated until it intersected the abscissa at zero altitude, point P This method of determination was used to check the height of the signal zone of the SDA array when the power to the array was increased to give a zone height of 20,000 feet The airplane used for the test flights was not capable of flying to 20,000 feet, and it was necessary to resort to this method of extrapolation to determine the zone height The maximum deflection of the recorder was determined for a test flight on the SDA signal zone at an altitude (13,000 feet) sufficient to insure linear operation of the receiver This deflection was plotted on figure 26, point F A straight line was drawn through points P and F (curve B) and extended until it intersected the light time axis The altitude at this point of intersection, 21,500 feet, was the extrapolated height of the SDA signal zone Other values of recorder deflection versus altitude were determined by flight test on this signal zone up to 13,000 feet, and the curve is shown in solid line from point F to the limiting abscissa of recorder deflection For all values of recorder deflection, which are directly proportional to field strengths, the ratio of altitudes for the straight portions of curves A and B is constant, thus substantiating the inverse law relating the attenuation of the electric field with distance along a constant elevation angle

The signal zones received from the SDA marker and the ID marker for altitudes up to 10,000 feet above ground are shown in figure 27 These patterns were obtained under conditions of negligible wind Flights were made in the east-west direction over both markers The ratios of the widths of the patterns at several altitudes are tabulated in figure 27

Figure 28 shows the same patterns as figure 27, except that the pattern for the SDA marker has been extended to 20,000 feet above ground, i e , twice the height of the ID marker The current in the dipoles of the SDA antenna was raised to twice the value which existed at the time the data for figure 27 were obtained Test flights were then made on both Z markers up to and including an altitude of 13,000 feet These test flights confirmed the data plotted in figure 28 From these patterns it can be seen that the SDA marker zone is narrower than the present Z marker zone below 5,700 feet, even though its maximum height is twice that of the present Z marker The ratios of zone widths up to 5,000 feet are tabulated in figure 28

The increase in width of the signal zones of both markers for parallel flights to each side of the marker antennas at an altitude of 500 feet above ground is shown in figure 29 In these two tests the receiver sensitivity was adjusted to give a signal zone height of 10,000 feet The elongated pattern for the SDA Z marker is also shown for an altitude of 3,000 feet The parallel chord flights on the ID Z marker were not made in a truly east-west direction since the dipoles of this marker are aligned 30° clockwise from the true north-south, east-west direction

During these flights in NC–17 it was discovered that the receiving antenna had a greater pick-up on the right side than on the left side of the airplane for the same angle of reception with respect to a vertical plane through the receiving antenna It was, therefore, necessary to average the data obtained and to compensate for this difference in pick-up as well as for differences in signal widths computed for flights in opposite directions The composite averages for both the SDA and the ID markers are shown in figure 29 The area within the patterns represents the horizontal area at an altitude of 500 feet over which a signal equal to or greater than a value sufficient to light the signal lamp will be received for parallel flights to either side of the station and perpendicular to the major axes of the elliptical patterns The average width of the curves in the major directions is as follows for the SDA marker, 1,900 feet, for the ID marker, 2,800 feet, a ratio of 0 68 The fact that the ratio of the average distance in the major directions is not so low as the width of the signal zones at 500 feet, as shown in figure 27, can be accounted for by the slightly greater degree of symmetry of the ID marker array as explained in the Theoretical Discussion The ratio of the major to the minor axis at

a 500-foot altitude for the SDA Z marker is 4 75, and for the ID marker it is 4 5 This is further substantiation of the differences in symmetry

If the limit of the major axis of the elongated pattern were plotted for various altitudes, it would have the form of the $f_B(\theta)$ curves of figures 2 and 3 If the receiving pattern of the airplane antenna were uniform for various angles in a plane normal to the antenna axis, the ratio of the width of the $f_B(\theta)$ curve to the width of the $f_A(\theta)$ curve at various relative altitudes would give a close approximation of the ratio of the major to minor axes of the elongated patterns at those altitudes Actually, the ratios as measured are slightly greater than that predictable by the vertical patterns in figures 2 and 3 From these tests and calculations made of the airplane receiving patterns it can be concluded that the width of the signal zone and the elongation of the pattern for parallel flights to one side of the Z marker is also a function of the characteristics of the receiving antenna on the airplane

The results of test flights made during a time of high winds aloft are shown in figure 30 These flights were made during the time the unsymmetrical array was being used The crab angle was 17 5° and the wind velocity averaged 50 miles per hour between 2,000 and 10,000 feet above ground It will be noted that the enlargement of the pattern is more pronounced in the case of the ID marker than in the case of the SDA marker A comparison of figures 27 and 30 shows that even under this extreme crab angle the SDA marker pattern is only slightly larger than the ID marker pattern shown in figure 27, which was obtained under the most favorable wind conditions The zone width due to crabbing is increased because of the increased pickup of the receiving antenna as the axis of the antenna is turned away from the direction of flight It is to be expected that the enlargement of the symmetrical SDA Z-marker pattern due to crabbing will be slightly greater than that for the unsymmetrical SDA Z-marker, due to its larger $f_B(\theta)$ pattern, but still not as great as that for the ID Z-marker

The horizontal cross-sectional patterns of radial flights over the marker are not circular at all altitudes This may be ascribed to the fact that the received field along different radii over the marker is the vector resultant of the fields from both arrays in quadrature time phase Horizontal patterns were taken on radial flights at altitudes of 500, 2,000, and 5,000 feet (fig 31) The height of the SDA marker was 10,000 feet during these tests The 2,000-foot and 5,000-foot patterns are practically square The 500-foot pattern is practically circular

486924—43——3

CONCLUSION

It has been shown that the SDA antenna system possesses a number of distinct advantages over that of the present Z marker, viz,

(1) The marker will provide a more accurate position fix because the zone is considerably less at all altitudes

(2) The marker zone can be extended to 20,000 feet altitude without modification of the present transmitters Under these conditions the zone will be narrower than the present type of marker for all altitudes up to 5,700 feet and will be only 54 5 percent as wide at 1,000 feet

(3) The broad marker zone normally obtained on flights off to one side of the antenna is appreciably reduced, resulting in a more accurate fix over the radio range station

(4) Under flight conditions involving large crab angles the marker zone is considerably smaller than with the present type of marker

(5) The antenna system is easy to adjust and will provide a reliable and stable Z-marker zone under rain, snow, and sleet conditions

(6) The radiating elements are simple in design, easy to adjust, and are adapted to quantity production They may be assembled in the factory as prefabricated units ready for field installation

It also has been shown that highly directive radiator patterns with negligible minor lobes may be obtained with collinear, cophased dipoles using spacings greater than 180°, provided that the dipole currents are proportioned in accordance with the coefficients of successive terms of the binomial expansion $(a+b)^n$, where $(n+1)$ is the number of dipoles constituting the array

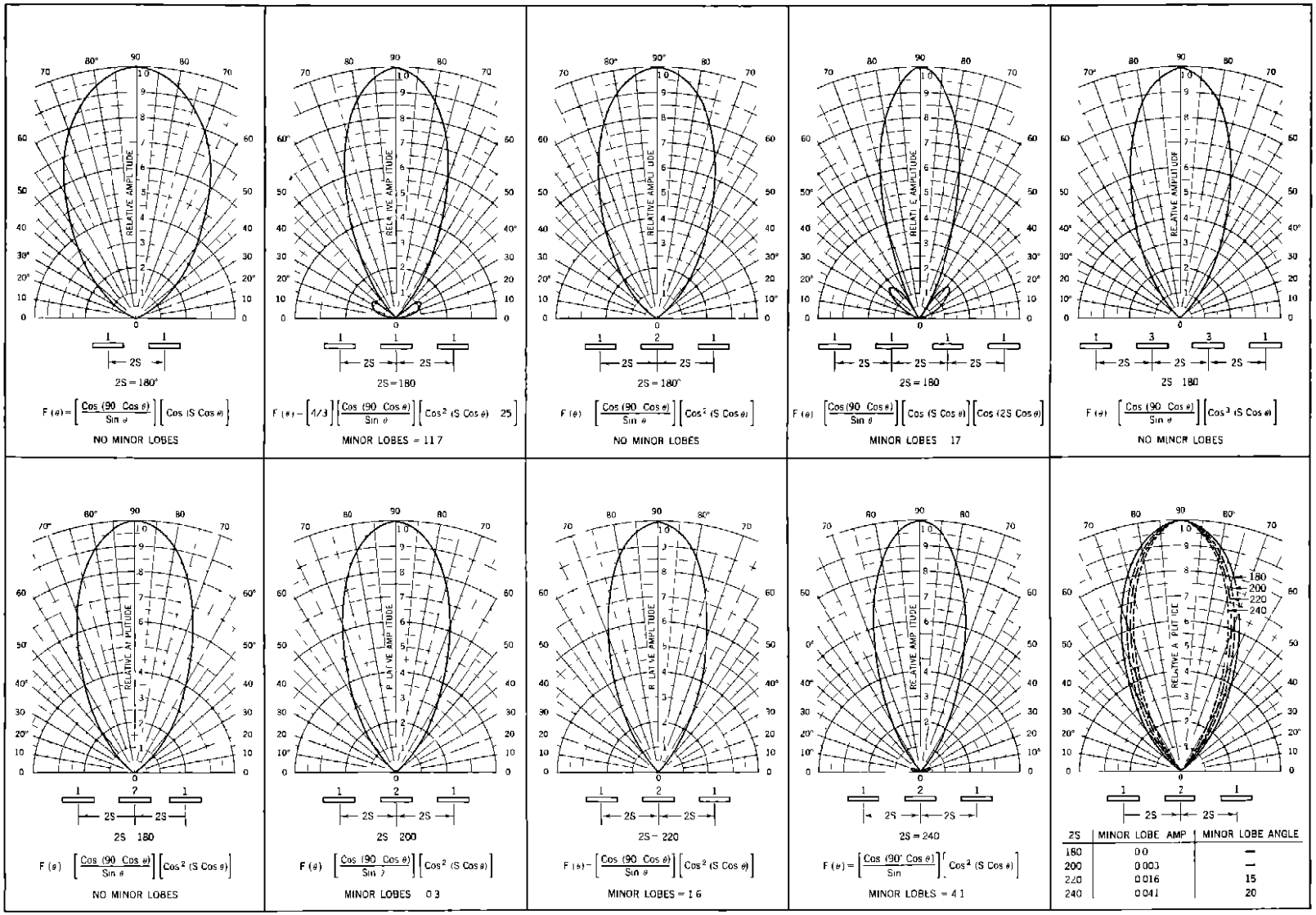

Figure 1 Free space vertical radiation patterns for various numbers of elements, current ratios, and spacings

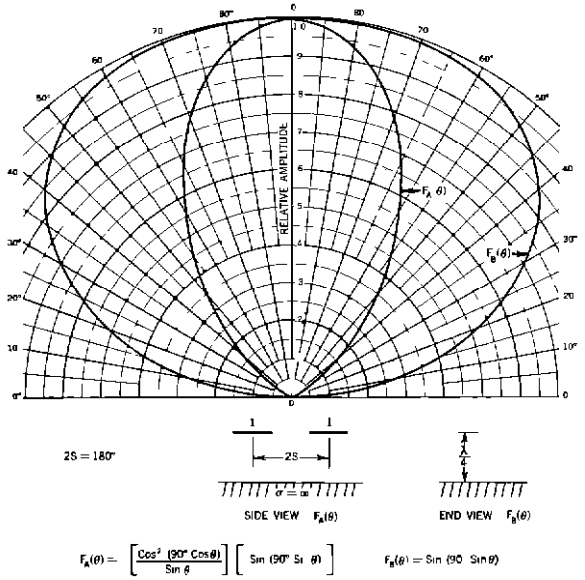

Figure 2 —Vertical radiation patterns—Present Z-marker array

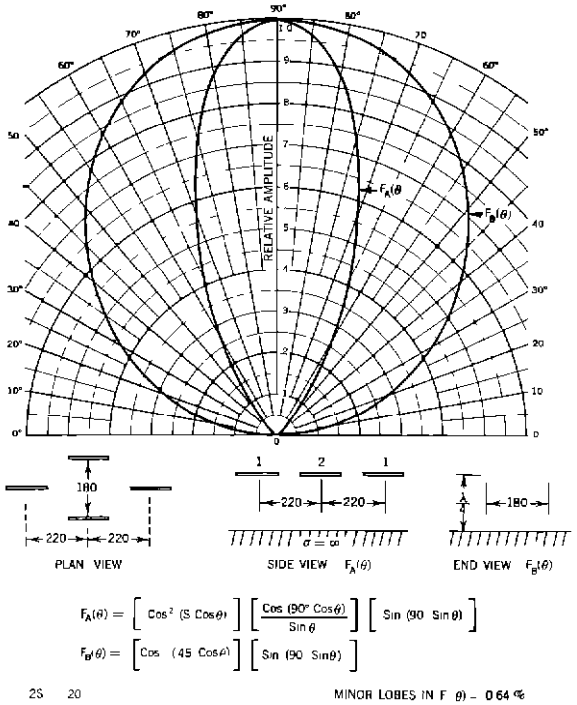

Figure 3 —Vertical radiation patterns—SDA array

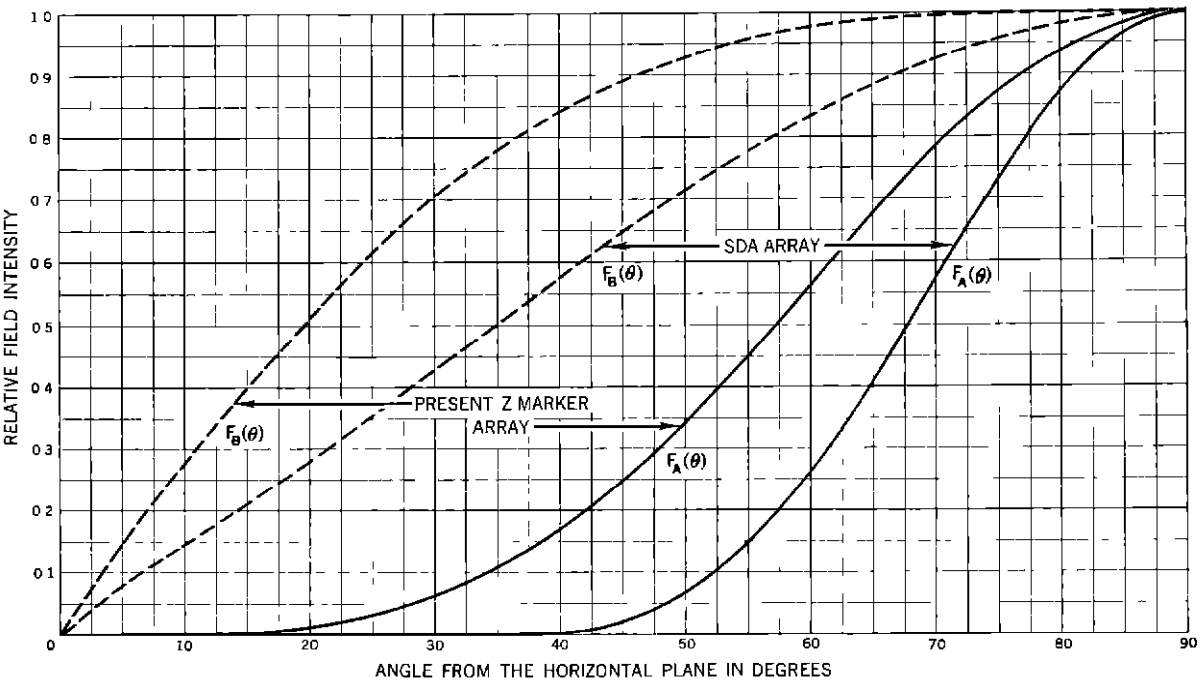

Figure 4 —Vertical radiation patterns –Antennas a quarter wave above perfect earth

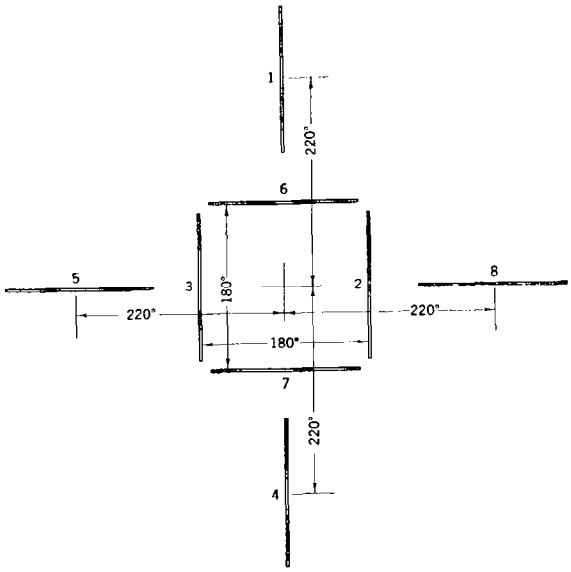

Figure 5.—Plan layout of the SDA Z-marker antenna.

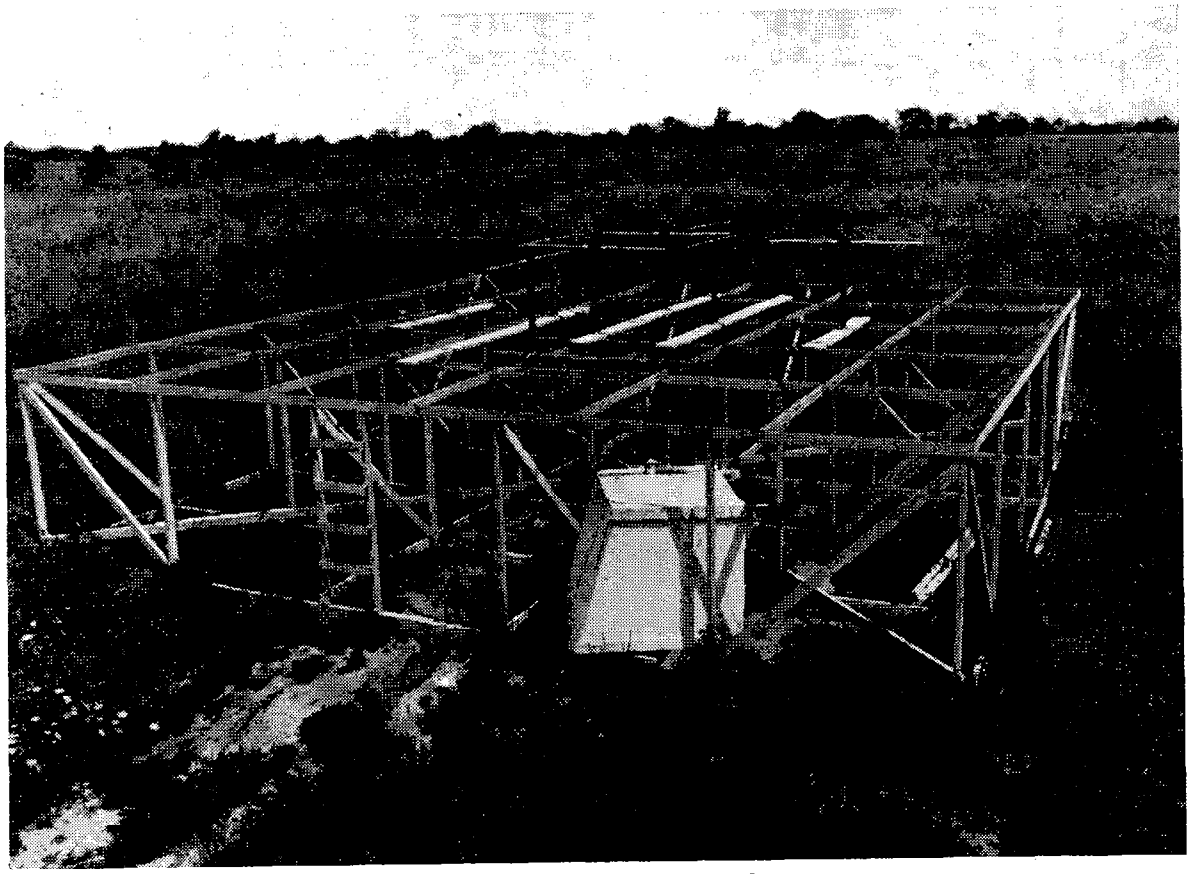

Figure 6.—SDA Z-marker antenna layout.

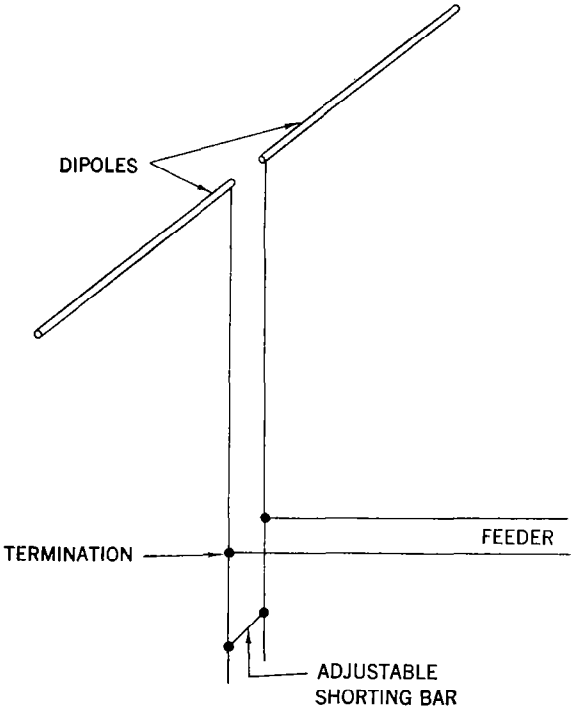

Figure 7.—Dipole antenna and tuning section.

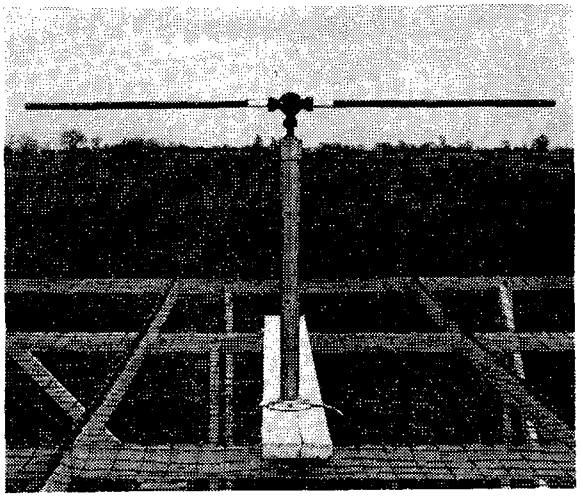

Figure 8.—Dipole and support.

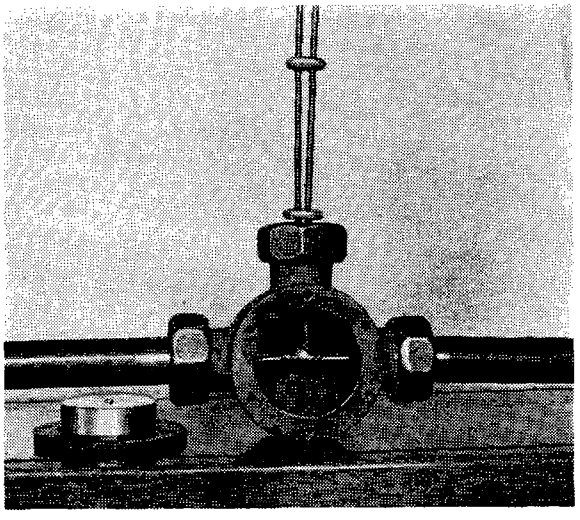

Figure 9.—Butt weld.

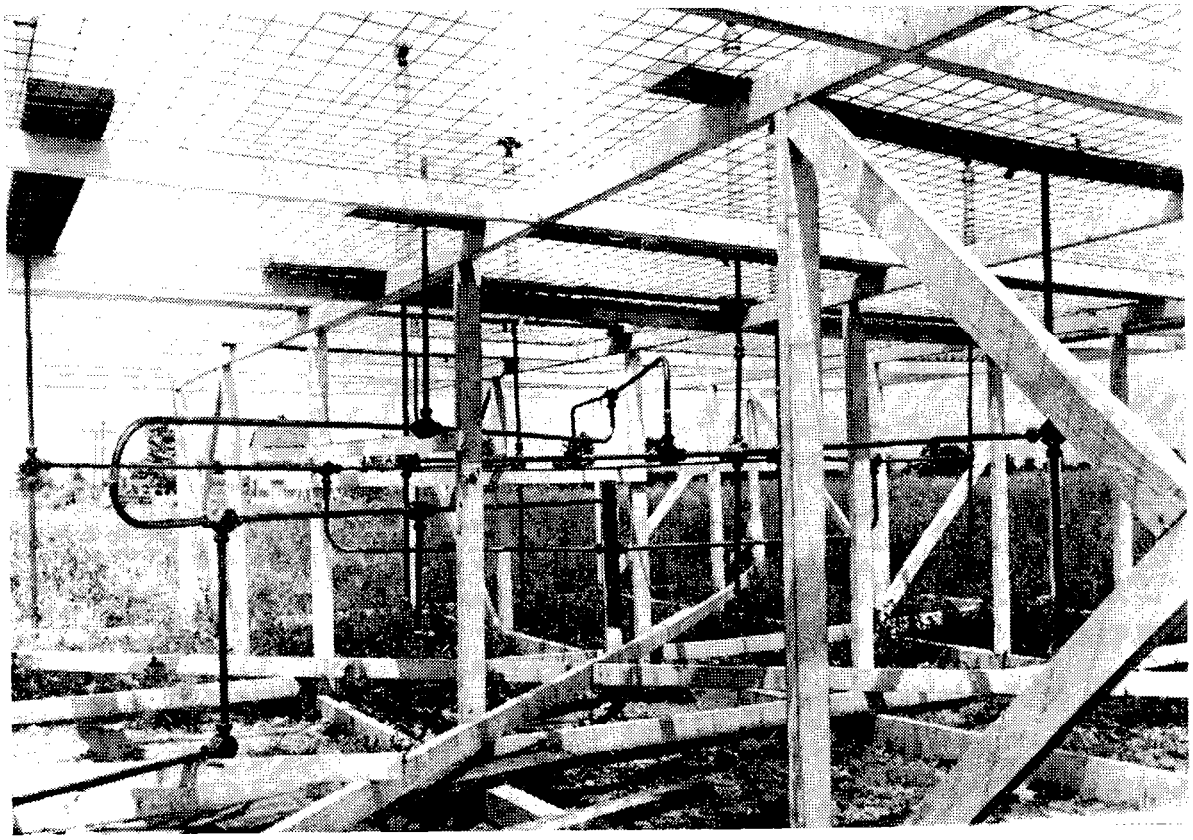

Figure 10.—SDA Z-marker antenna feeder system.

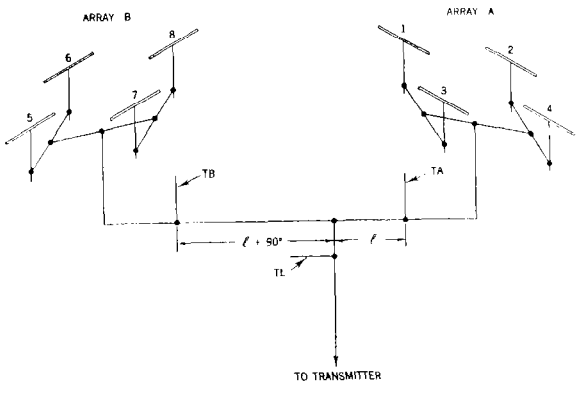

Figure 11.—Schematic diagram of SDA Z-marker antenna system.

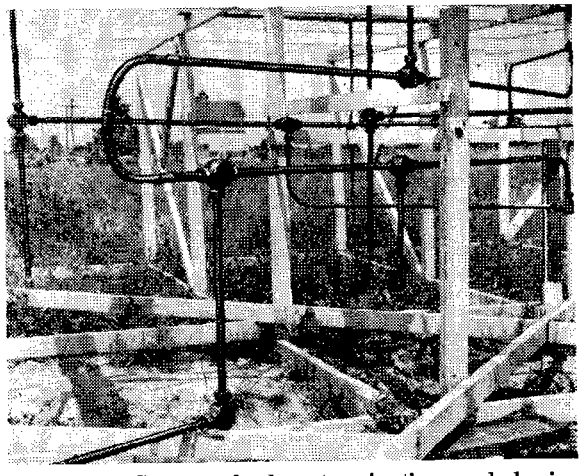

Figure 12.—Common feeders, terminations and phasing section.

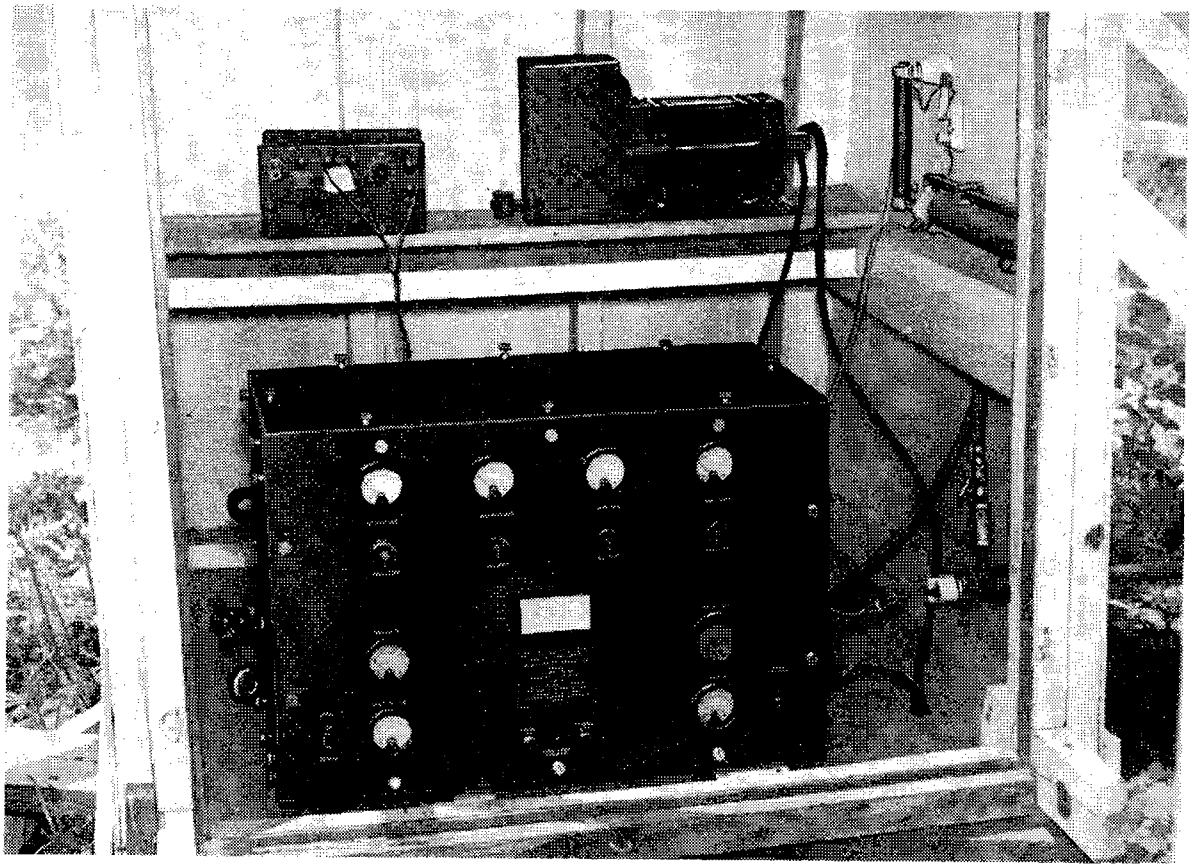

Figure 13.—UHF inner marker transmitter, audio oscillator and voltage regulator.

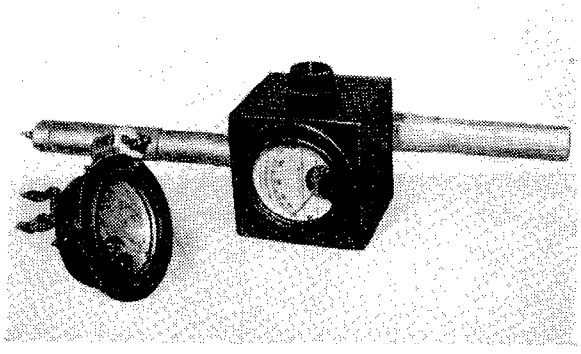

Figure 14. Antenna meter and probe detector.

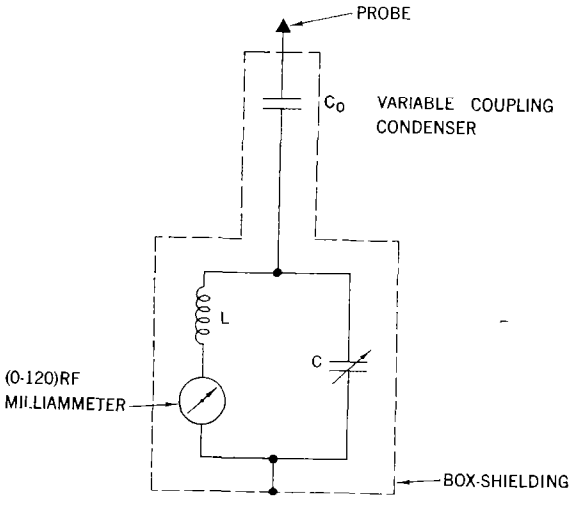

Figure 15.—Schematic diagram of probe detector.

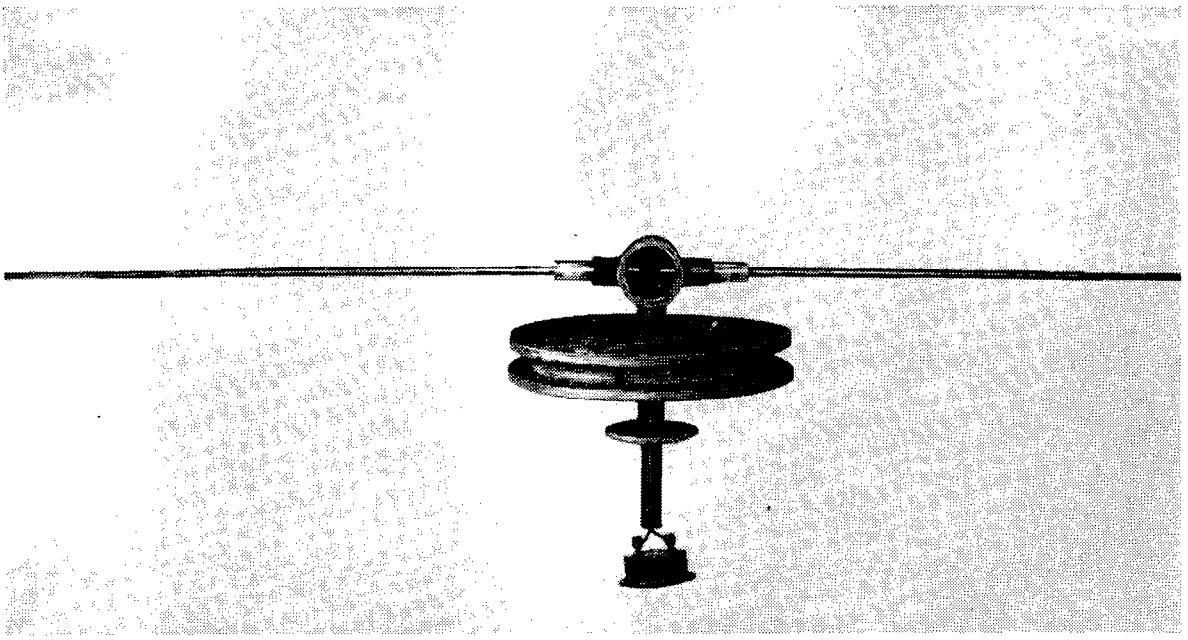

Figure 16.—Pick-up dipole.

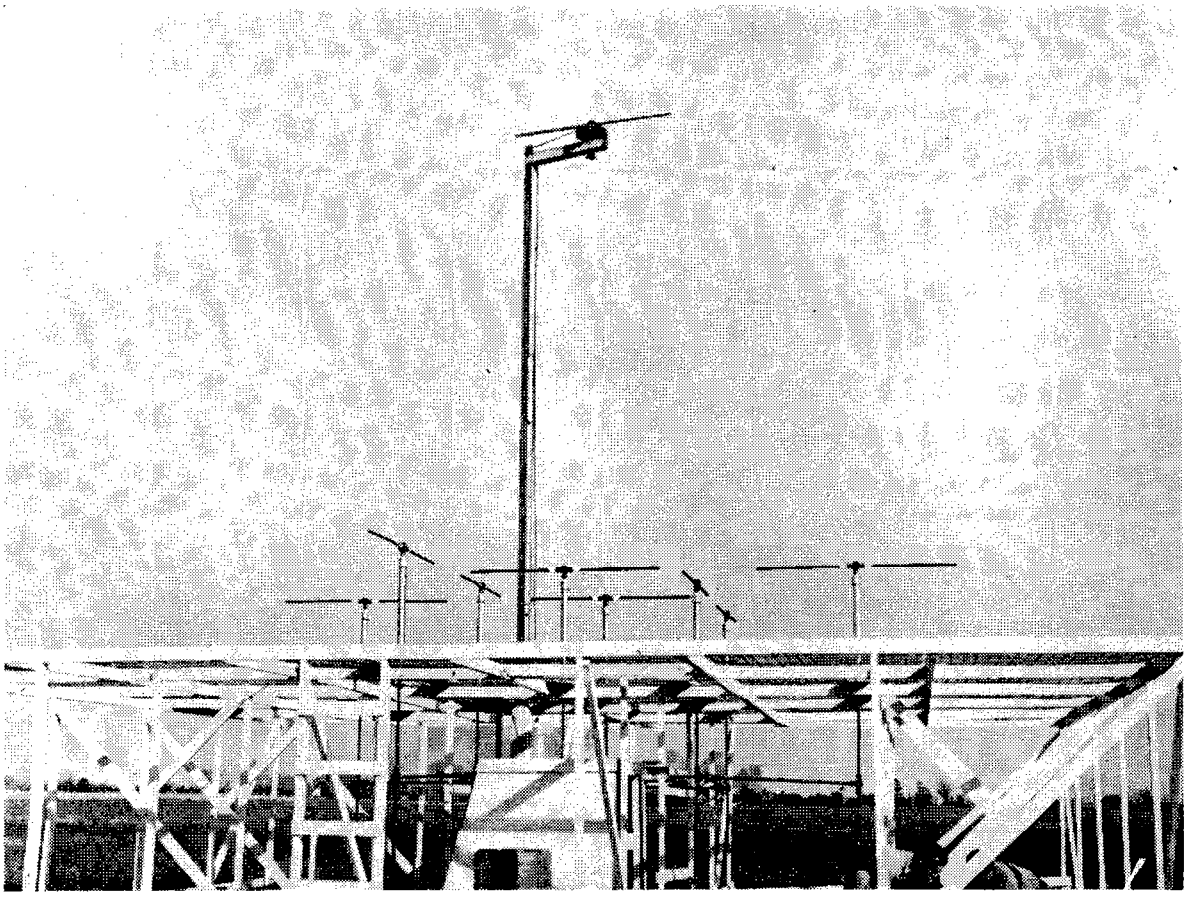

Figure 17.—Pick-up dipole in place.

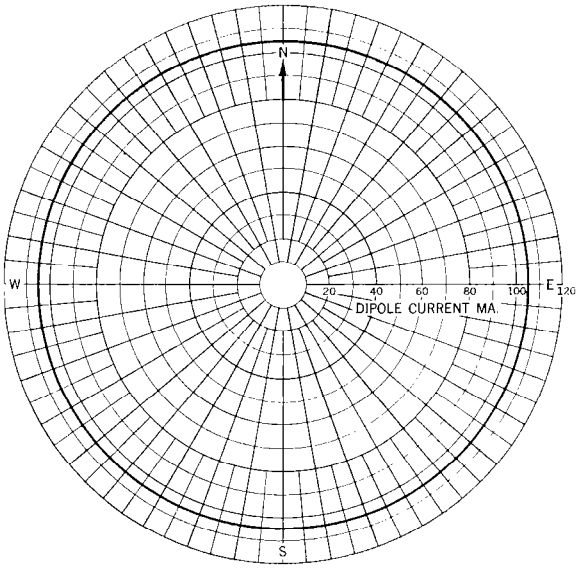

Figure 18. —Observed currents in pick-up dipole for various angular positions in the horizontal plane above the antenna.

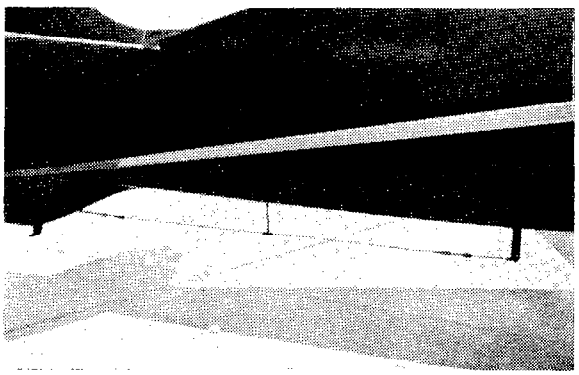

Figure 19.—Marker receiving antenna on NC–17.

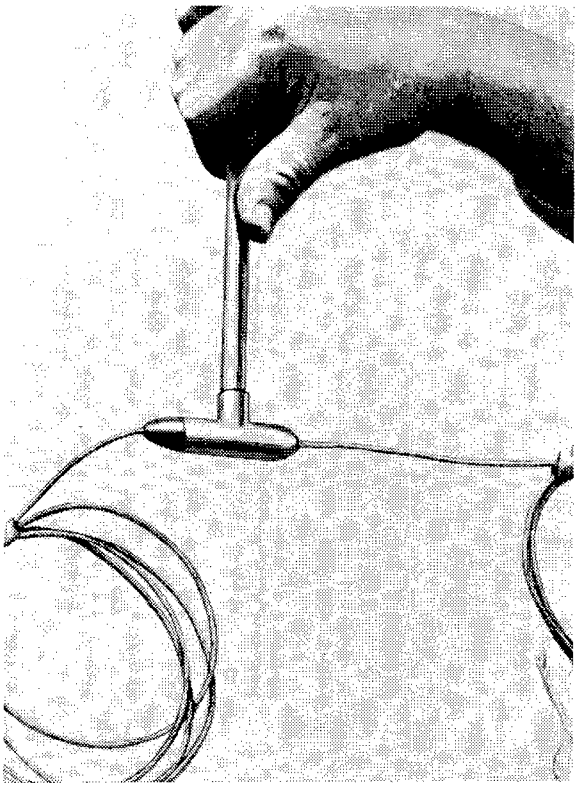

Figure 20. Close-up of marker receiving antenna.

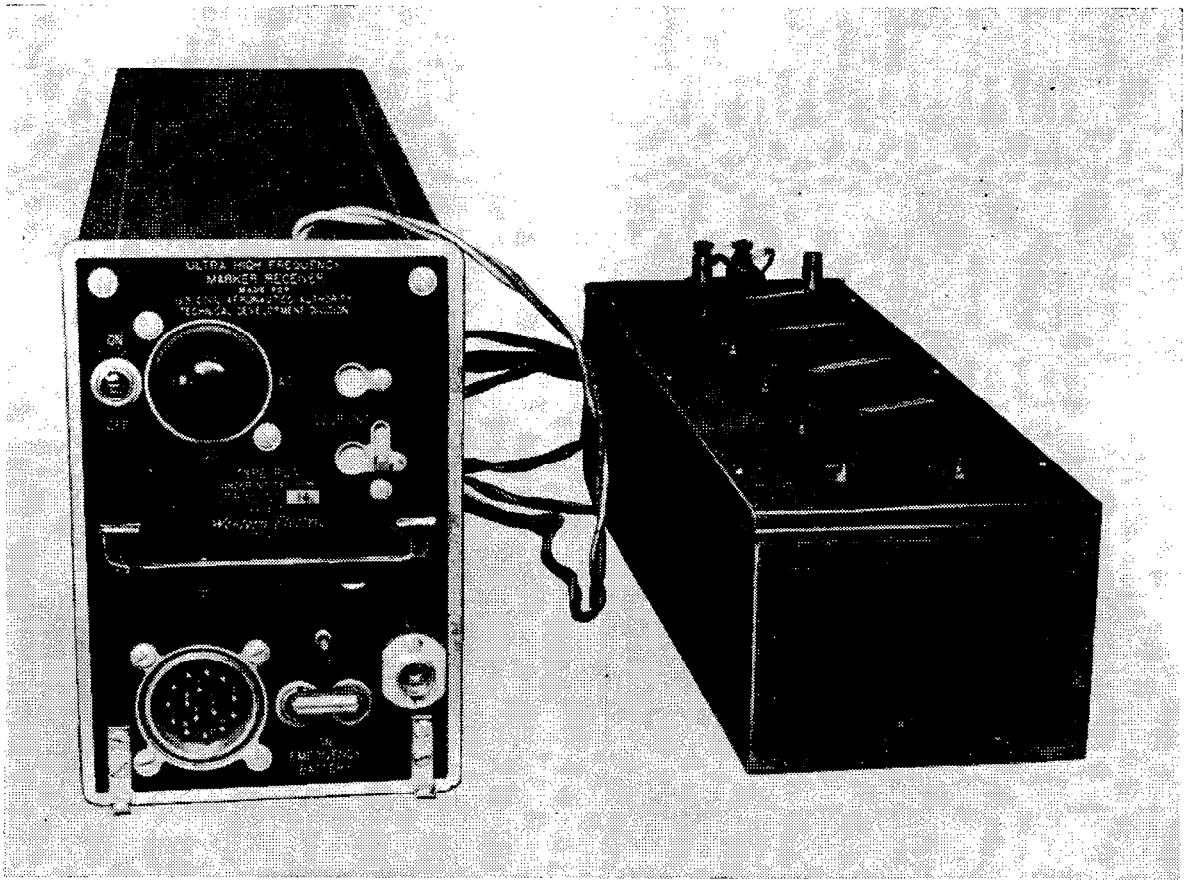

Figure 21.—UHF marker receiver and decade resistance box.

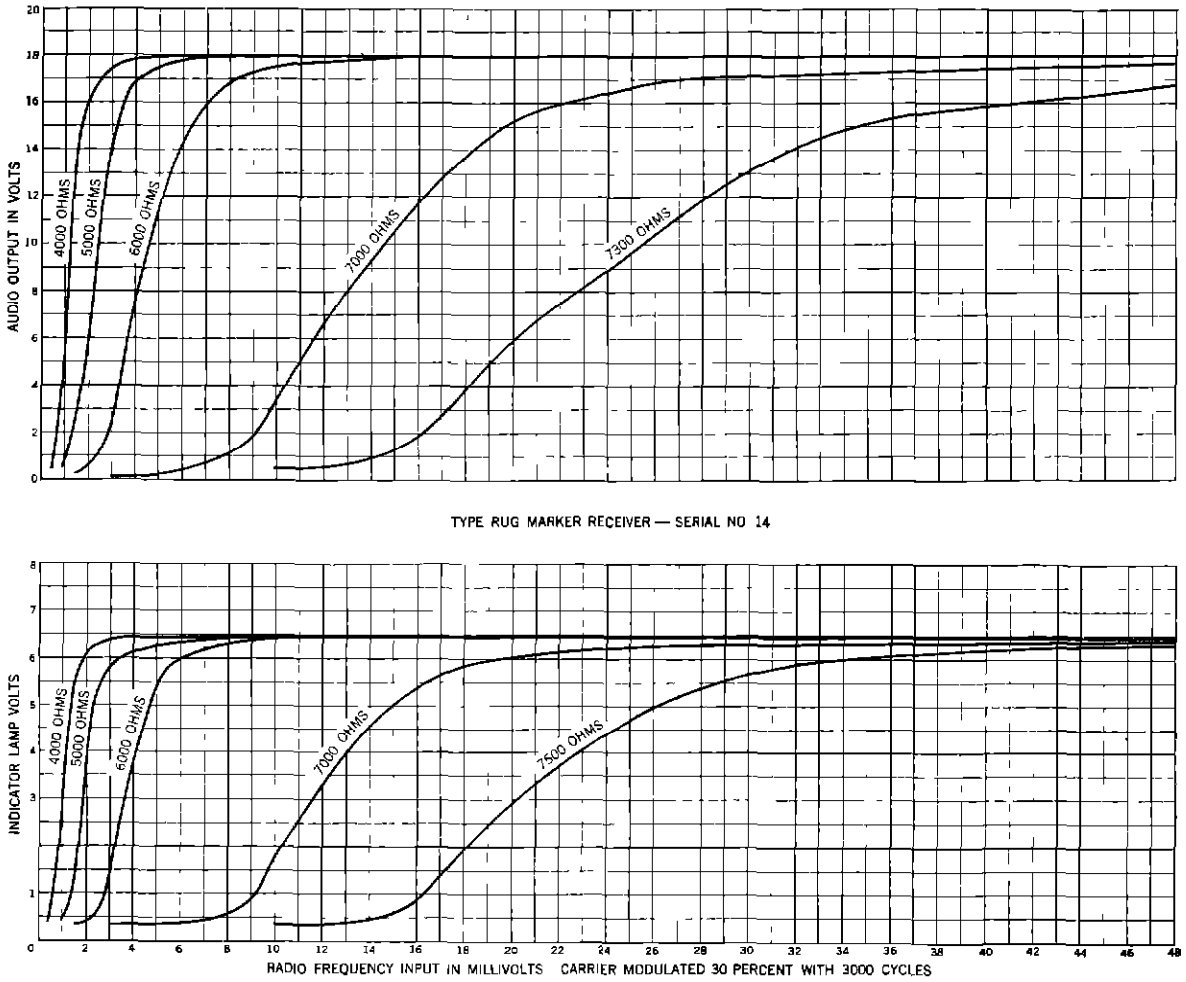

Figure 22 —UHF receiver calibration type RUG, serial No 14 Audio and indicator lamp volts vs radio-frequency input for various values of first intermediate-frequency stage cathode resistance

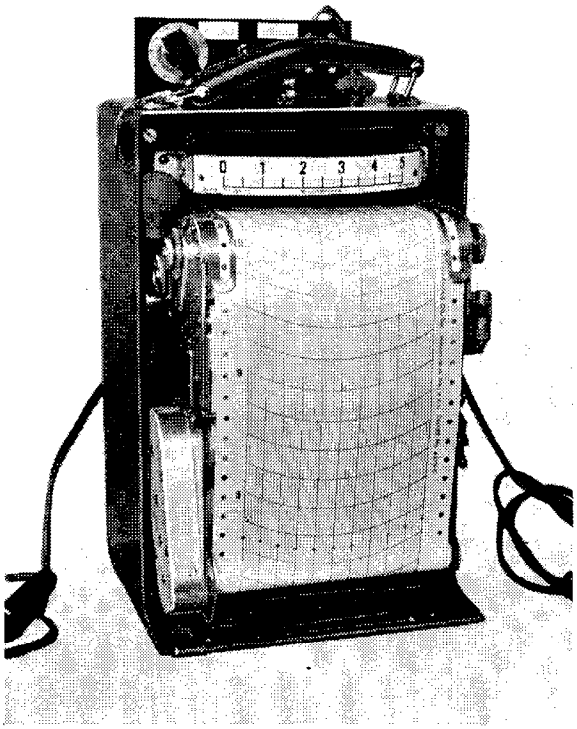

Figure 23. —Esterline-Angus graphic meter.

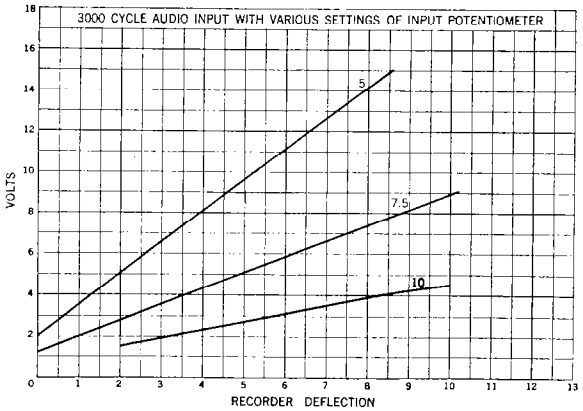

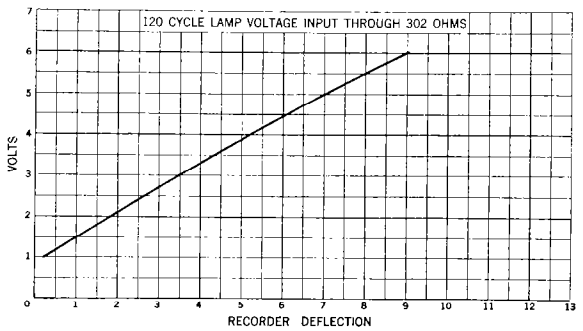

Figure 24.—Calibration of Esterline-Angus graphic meter, model AW, serial No. 28883, deflection vs. input volts.

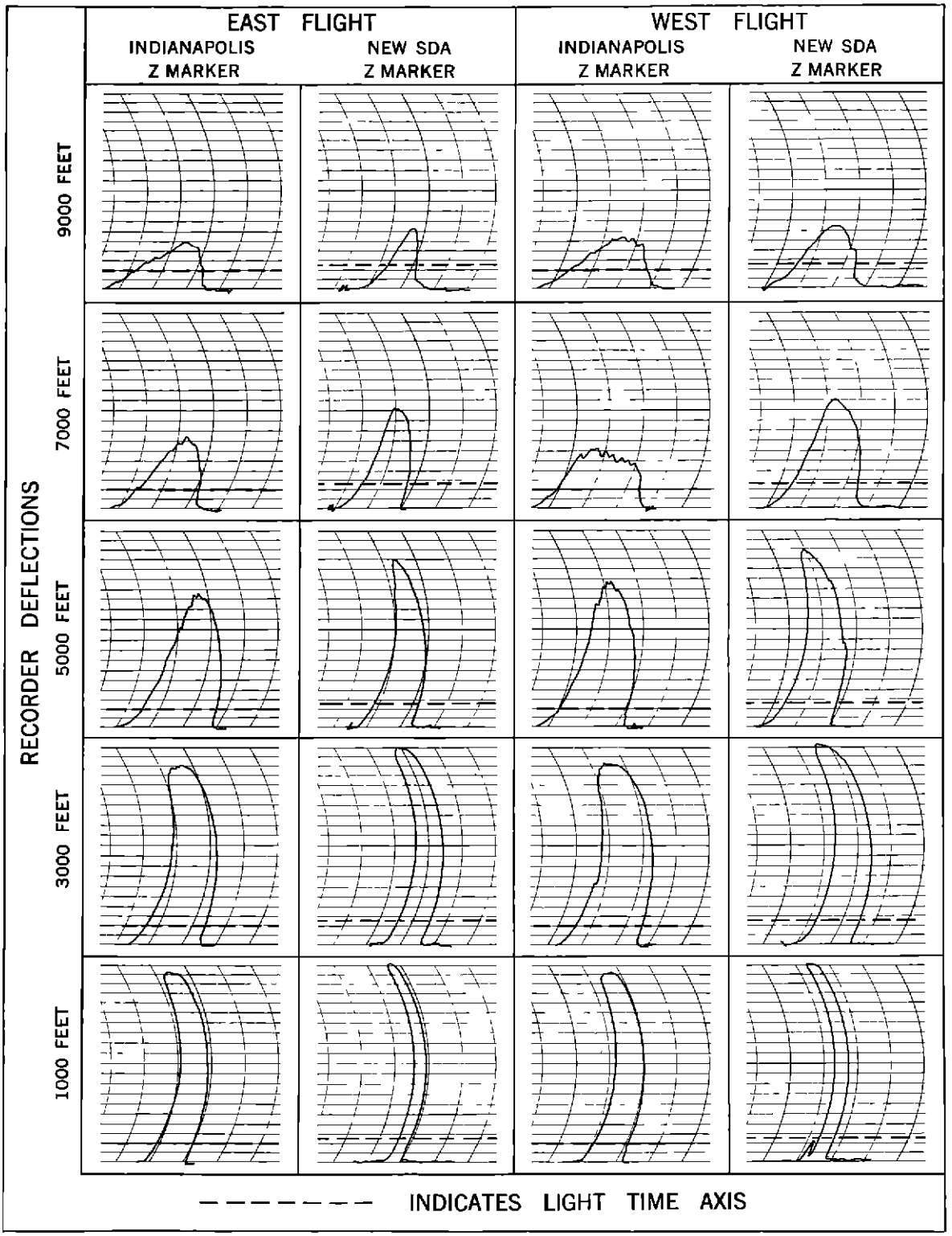

Figure 25 Copies of actual flight recordings of the present Z-marker and the new SDA array at various altitudes showing comparisons of each array under identical flight conditions

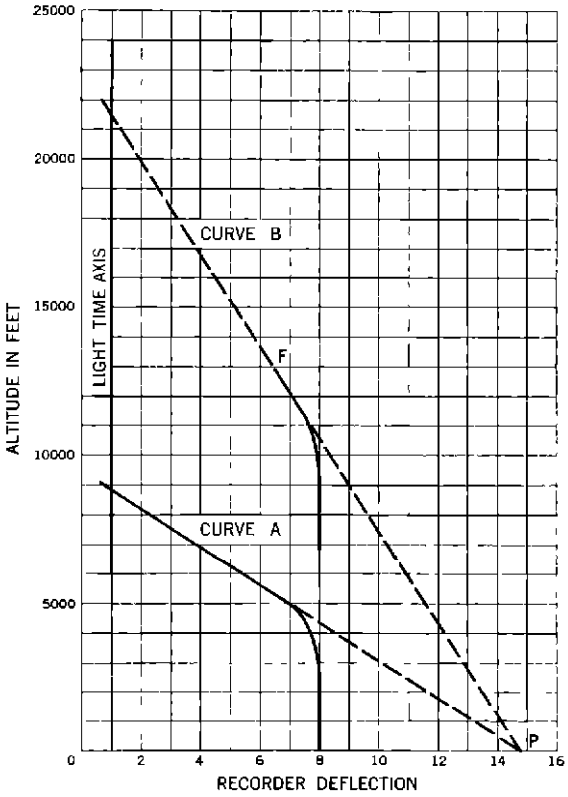

Figure 26 —Signal zone height determination

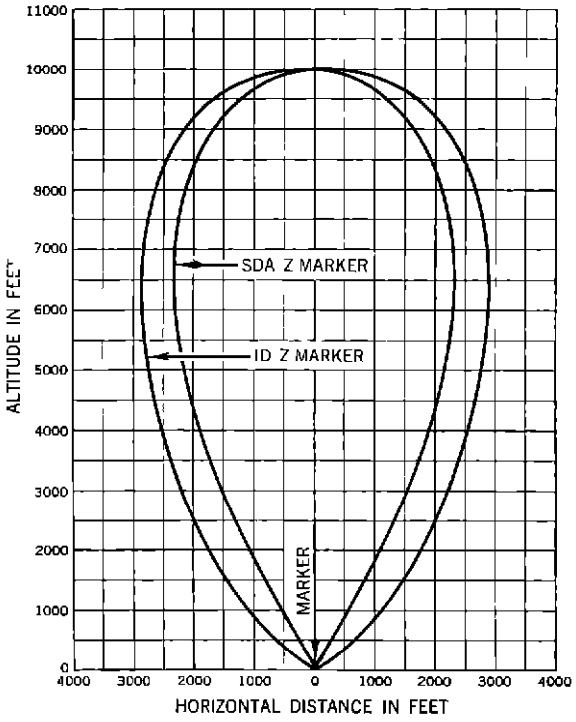

WIDTH OF SDA Z MARKER COMPARED TO ID Z MARKER IN PERCENT

ALTITUDE	PERCENT
7000	78 5
6000	78 5
5000	77 0
4000	74 0
3000	65 5
2000	59 0
1000	50 0
500	46 0

Figure 27 —Z-marker patterns—Measured zone widths for 10,000-foot signals

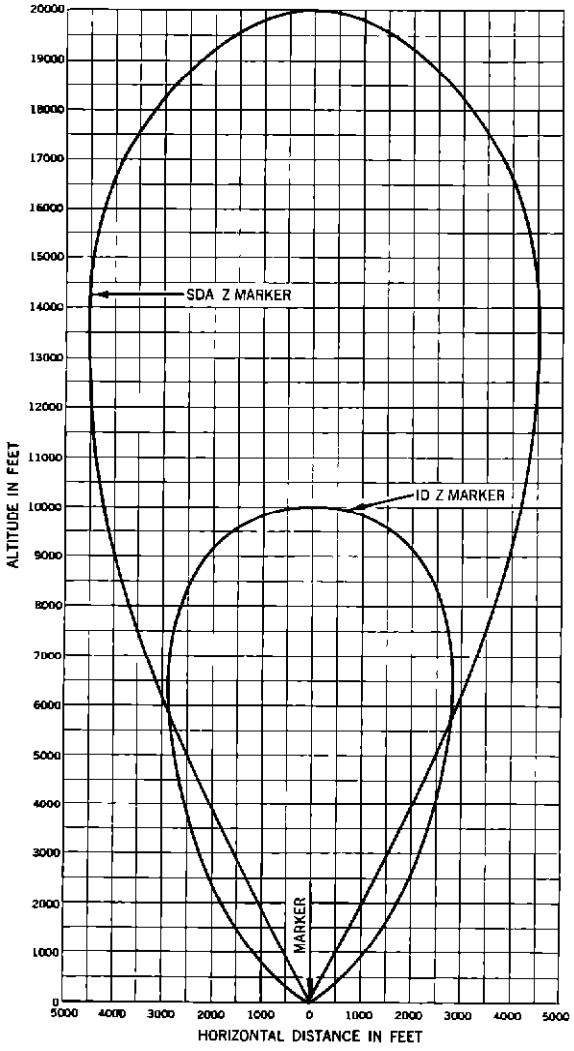

WIDTH OF SDA Z MARKER COMPARED TO ID Z MARKER IN PERCENT

ALTITUDE	PERCENT
5000	93 8
4000	83 7
3000	74 5
2000	64 0
1000	54 5
500	55 0

Figure 28 —Z-marker patterns—Measured zone widths for 10,000 and 20,000-foot signals

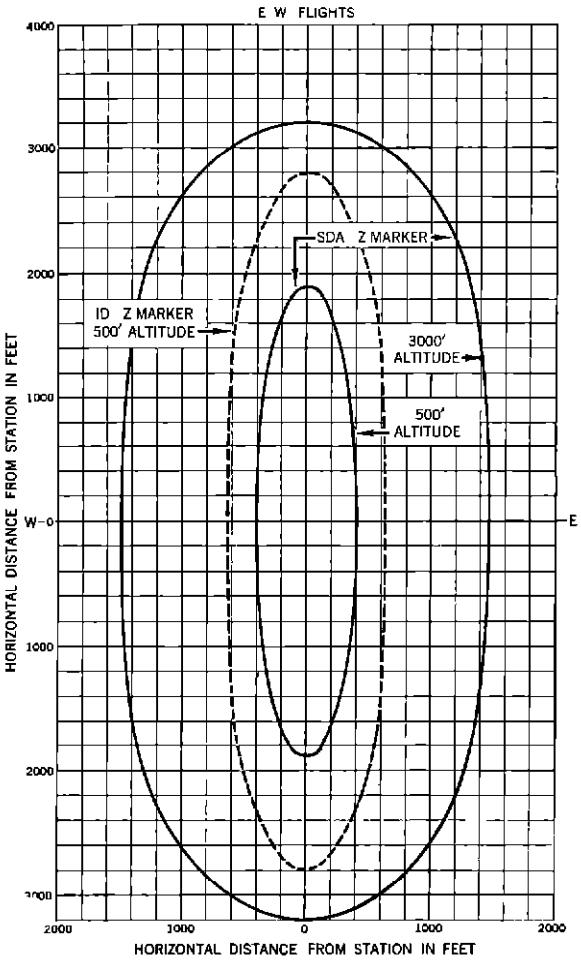

Figure 29 —Parallel chord patterns of Z-markers for for 10,000-foot signal

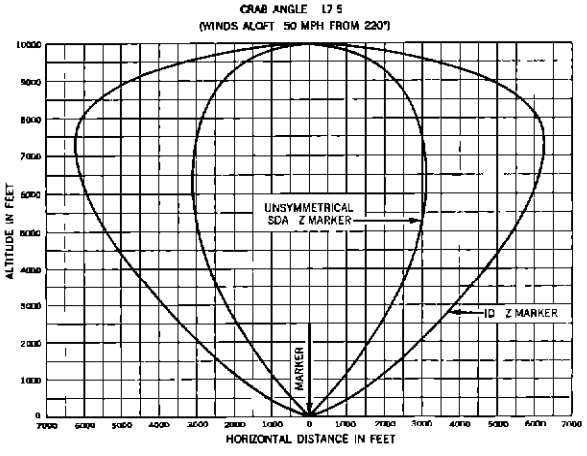

Figure 30 —Z-marker patterns under condition of large crab angle

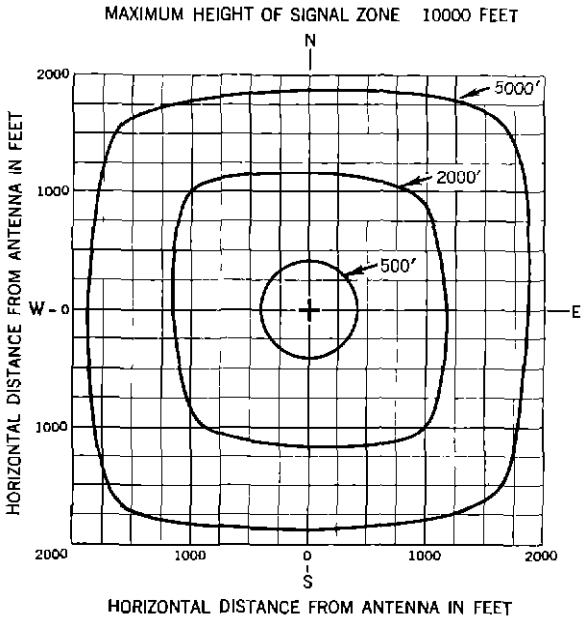

Figure 31 — Horizontal pattern of SDA Z-marker for radial flights at altitudes of 500, 2,000, and 5,000 feet

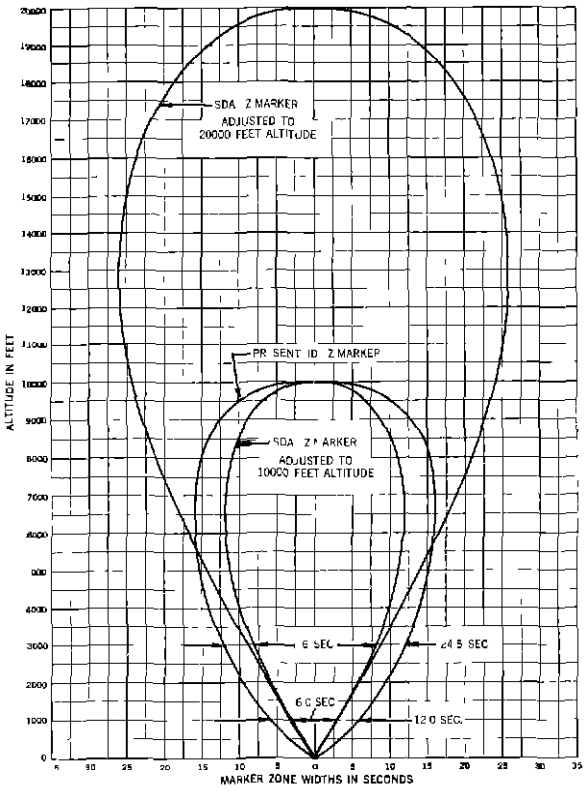

Figure 32 Z-marker patterns—Width in seconds—for 120 miles-per-hour ground speed